

Benchmarking Pretrained Molecular Embedding Models For Molecular Representation Learning

Mateusz Praski*, Jakub Adamczyk*, Wojciech Czech

Faculty of Computer Science, AGH University of Krakow, Cracow, Poland
{praski,jadamczy,czech}@agh.edu.pl

Abstract

Pretrained neural networks have attracted significant interest in chemistry and small molecule drug design. Embeddings from these models are widely used for molecular property prediction, virtual screening, and small data learning in molecular chemistry. This study presents the most extensive comparison of such models to date, evaluating 25 models across 25 datasets. Under a fair comparison framework, we assess models spanning various modalities, architectures, and pretraining strategies. Using a dedicated hierarchical Bayesian statistical testing model, we arrive at a surprising result: nearly all neural models show negligible or no improvement over the baseline ECFP molecular fingerprint. Only the CLAMP model, which is also based on molecular fingerprints, performs statistically significantly better than the alternatives. These findings raise concerns about the evaluation rigor in existing studies. We discuss potential causes, propose solutions, and offer practical recommendations.

Introduction

The translation of molecular structures into information-rich numerical representations is a cornerstone of modern chemoinformatics and a critical step for harnessing machine learning in drug discovery and materials science. Molecular representation learning has emerged as a powerful paradigm, moving beyond handcrafted descriptors to automatically learn salient features from molecular data. Recently, the field has seen a surge in the development of pretrained molecular embedding models. This trend mirrors the transformative impact of representation learning in other scientific domains, where models are pretrained on vast unlabeled datasets to produce powerful general-purpose embeddings. Notable successes include models based on self-supervised learning (SSL), such as DINO (Caron et al. 2021) and DINOv2 in computer vision, Sentence Transformers and TS-DAE (Wang, Reimers, and Gurevych 2021) for dense text representations in NLP, and multimodal architectures such as CLIP and BLIP-2 that connect images and text. Inspired by these advances, molecular models are similarly trained on massive chemical databases to generate universal embeddings.

*These authors contributed equally.
Copyright © 2026, Association for the Advancement of Artificial Intelligence (www.aaai.org). All rights reserved.

This study focuses specifically on evaluating these static embeddings rather than the alternative approach of task-specific fine-tuning. The rationale is threefold: first, we probe the fundamental knowledge encoded during pretraining and assess the intrinsic generalization capabilities of the learned representations themselves; second, to evaluate their utility in unsupervised applications such as molecular similarity searching and clustering, where embeddings are used directly; and third, to address the challenge of low-data learning, a common scenario in chemistry where fine-tuning complex models would lead to severe overfitting.

The proliferation of pretrained models, each with unique architectures and pretraining objectives, has created a pressing need for their systematic and rigorous evaluation. The absence of standardized and comprehensive benchmarking of the embeddings themselves hinders the ability to make informed decisions about model selection and impedes further progress in the field. To address this critical gap, this paper presents a comprehensive benchmarking study of state-of-the-art pretrained molecular embedding models. We evaluated their performance in a wide range of molecular representation learning tasks, providing a clear and objective comparison of their capabilities.

Our findings challenge the prevailing view of progress in this domain. We reveal that despite their sophistication, modern pretrained models struggle to outperform traditional, much simpler methods. Specifically, we find that traditional chemical fingerprints often remain the top-performing representations. Furthermore, embeddings derived from Graph Neural Networks (GNNs) generally exhibit poor performance across the tested benchmarks. Although pretrained transformers that incorporate a strong chemical inductive bias perform acceptably, they do not demonstrate a definitive advantage. These results suggest that significant progress is still required to unlock the full potential of deep learning for universal molecular representation.

Molecular Embedding Approaches

Molecular representation learning has long been a central focus in chemoinformatics and molecular machine learning, encompassing a wide range of techniques and approaches. Classical methods rely on deterministic feature extraction techniques, exemplified by molecular fingerprints. Subse-

quent advances in neural networks for molecular data have enabled transfer learning from large pretraining datasets through embedding models. These approaches can be categorized according to their input modality, architecture, and pretraining objectives.

Molecular graphs, based on atom and bond structures, provide a natural representation of chemical compounds. In most cases, models use the topological (2D) graph, while ignoring the spatial (3D) conformation, as 3D structures are expensive and often difficult (or even impossible) to compute. However, the 2D graph retains much of the practically useful information. Architectures that operate on this representation include Graph Neural Networks (GNNs) and graph transformers.

Compounds can also be serialized as SMILES or SELFIES strings, which are the standard formats for molecular datasets. Many models inspired by natural language processing (NLP) operate directly on these textual representations, primarily using transformer-based architectures.

Finally, there are hybrid models that utilize multimodal representations or pretraining objectives, for example, incorporating the inductive biases of graph-based representations into more scalable and easily trainable text-based models.

In the following sections, we describe a range of molecular embedding models that encompass these different approaches, all of which have been implemented for benchmarking in this study. Model selection was based on the availability of code and pretrained weights, as well as the ability to successfully run the code. Due to space limitations, the following descriptions omit some details, such as specific model variants or pretraining datasets. We refer interested readers to the original publications for further information.

Molecular fingerprints

Molecular fingerprints are feature extraction methods based on identifying small subgraphs within a molecule and detecting their presence or counting their occurrences, yielding binary and count variants, respectively. They can be broadly classified into substructural and hashed types (Adamczyk and Ludynia 2024). Substructural fingerprints detect predefined patterns, such as functional groups or ring systems, that are typically determined by expert chemists. Hashed fingerprints, on the contrary, define general shapes of extracted subgraphs, convert them into numerical identifiers, and hash them using a modulo function into a fixed-length output vector. Common examples include circular neighborhoods in Extended Connectivity FingerPrint (ECFP) (Rogers and Hahn 2010), paths of length 4 in the Topological Torsion (TT) (Nilakantan et al. 1987), and the shortest paths between atom pairs in Atom Pair (AP) fingerprint.

Although not task-adaptive, hashed fingerprints remain widely used in cheminformatics and molecular machine learning due to their flexibility, computational efficiency, and consistently strong performance. In many cases, they continue to outperform more complex approaches, such as GNNs (Jiang et al. 2021; Baptista et al. 2022; Adamczyk and Czech 2024; Adamczyk, Ludynia, and Czech 2025).

Graph neural networks

Most Graph Neural Network (GNN) architectures follow a message-passing framework (Gilmer et al. 2017). The initial embedding of each atom consists of elementary chemical descriptors such as the element type or charge. In each GNN layer, an atom receives embeddings from its neighbors (messages) and updates its own embedding accordingly, incorporating this information. Most molecular GNNs also include bond features and embeddings in this process. To obtain a whole-molecule embedding, atom embeddings are aggregated using a readout function, such as a channel-wise average or sum. The message-passing mechanism integrates both functional and structural information about the molecule in an end-to-end learning framework.

Graph Isomorphism Network (GIN) (Xu et al. 2019) is one of the most widely used GNN architectures, as it was proven to be as expressive as the Weisfeiler-Lehman isomorphism test in distinguishing non-isomorphic graphs. GIN uses a two-layer multilayer perceptron (MLP) for atom embedding updates during message passing and employs sum readout. All GNN pretraining methods described below rely on a GIN backbone.

Context Prediction (ContextPred) (Hu et al. 2020) was proposed as an SSL pretraining procedure for message-passing GNNs. For each atom, a K -hop neighborhood subgraph is defined and encoded as a vector by the GNN that is being pretrained. A corresponding context subgraph, located between r_1 and r_2 hops away, is encoded by a separate GNN. The pretraining objective is binary classification with negative sampling, where the model learns to distinguish correct (positive) neighborhood-context pairs from randomly sampled (negative) ones.

GraphMVP (Liu et al. 2022) combines contrastive and generative SSL, aligning molecular 2D and 3D representations, i.e., topological graphs and conformations. These two views are encoded using GIN and SchNet (Schütt et al. 2018), respectively. In the contrastive setup, positive pairs consist of a molecule and its conformers, while the generative objective minimizes the variational autoencoder (VAE) loss between the two representations.

GraphFP (Luong and Singh 2023) introduces graph fragmentation for pretraining, employing both contrastive and predictive SSL. Frequent subgraph mining is used to decompose molecules into fragments. In contrastive learning, fragments and their constituent atoms form positive pairs, while atoms from unrelated fragments serve as negative pairs. The atom-encoding GNN is pretrained to generate atom-level embeddings (which can later be pooled), while a separate GNN encodes entire fragments. In addition, a predictive task is used to classify the presence of fragments, providing a multitask pretraining signal for the atom-encoding GNN.

MolR (Wang et al. 2022) also uses contrastive learning, but incorporates chemical reaction information. Positive samples are constructed from known reactant-product pairs in reaction databases, while negative samples are created by randomly shuffling these pairs. All molecules are encoded using the same GNN being pretrained, based on the TAG architecture (Du et al. 2017).

GEM (Fang et al. 2022) relies on predictive SSL, primarily using 3D molecular conformations. Pretraining tasks include predicting bond lengths, bond angles, and interatomic distances, with parts of the molecule masked as input. Additional auxiliary tasks involve predicting molecular fingerprint bits (MACCS and ECFP) based on the topological graph. Unlike the other architectures described above, which use only topological graphs at inference time, GEM requires 3D conformers as input, making both pretraining and inference computationally expensive due to the need for conformation generation.

Graph transformers

Graph transformer architectures extend self-attention mechanisms to molecular graphs, replacing or augmenting the localized message-passing of GNNs with global attention layers. Atoms are treated as tokens, and edges are encoded as pairwise biases injected into the attention scores, allowing information to propagate between any two atoms within a single layer. Compared to message-passing GNNs, this design more efficiently captures long-range dependencies and enables the incorporation of rich edge or distance features through additive or multiplicative attention biases.

GROVER (Rong et al. 2020) is a hybrid transformer-GNN model in which the attention heads are biased by cheminformatics-derived edge features. It is pretrained using two self-supervised tasks: multioutput regression (MTR), predicting eight physicochemical descriptors on masked subgraphs, and multioutput classification (MTC), predicting the presence of functional groups (structural motifs). The graph-level embedding is obtained by concatenating a [CLS] token with pooled atomic embeddings.

MAT (Maziarka et al. 2020) introduces distance-aware attention by incorporating adjacency and shortest-path kernels into the query-key dot product. Pretraining combines masked atom and bond prediction, analogous to masked language modeling (MLM) in NLP, with supervised regression on QM9 quantum-chemical properties, encouraging the encoder to learn both topological context and physicochemical properties.

R-MAT (Maziarka et al. 2024) builds on MAT by introducing relative positional encodings derived from graph distances and ring memberships, improving robustness to molecule size and graph sparsity. Inspired by GROVER, it uses subgraph masking as a pretraining objective, making it more challenging than single-atom masking of MAT, and resulting in superior performance.

Uni-Mol (Zhou et al. 2023) and its extended version, **Uni-Mol2** (Ji et al. 2024), apply graph transformers to 3D conformers using SE(3)-equivariant attention mechanisms. The encoder is jointly pretrained to reconstruct masked atoms, predict pairwise distances and angles, and distinguish positive from negative conformer-SMILES pairs. These objectives produce embeddings that integrate both molecular topology and 3D geometry.

Text transformers

Molecules serialized as SMILES (Weininger 1988) or SELFIES (Krenn et al. 2020) strings can be processed

directly using NLP-inspired architectures. Although pretraining can incorporate chemistry-specific biases, it is not strictly necessary, and the simplicity of NLP-derived pretraining is often a notable advantage of these models. In encoder-decoder architectures, only the encoder is used after pretraining to compute molecular embeddings.

Continous Data-Driven Descriptors (CDDD) (Winter et al. 2019) is an RNN-based architecture. It was trained using a purely text-based translation task, from random SMILES to canonical SMILES, calculated with RDKit (Landrum et al. 2025).

Chemformer (Irwin et al. 2022) is based on BART encoder-decoder transformer (Lewis et al. 2020), pretrained using denoising SSL objective. Given a SMILES string, it is first randomized (e.g., by starting at a different atom) and some tokens are randomly masked; the model is then trained to reconstruct the original SMILES.

MolBERT (Fabian et al. 2020) is an encoder-only transformer based on the original BERT architecture. It is pretrained using two objectives: masked language modeling (MLM), and multitask regression (MTR), in which the model predicts 200 physicochemical molecular properties computed with RDKit. This dual objective is intended to combine contextual learning from SMILES with molecular-level inductive biases.

ChemBERTa (Chithrananda, Grand, and Ramsundar 2020) uses a RoBERTa-style encoder-only architecture. The authors explore two distinct pretraining variants: one based solely on MLM and another based solely on MTR. The MTR-only variant is reported to be simpler to train compared to MolBERT, and achieves better performance than both the MLM variant and MolBERT combined objective.

MolFormer (Ross et al. 2022) is another encoder-only SMILES transformer. Its authors aim to further simplify pretraining by relying entirely on a large pretraining corpus (derived from PubChem and ZINC) and standard NLP procedures, rather than domain-specific architectural changes. The model is based on BERT, with modifications including linear attention and rotary position embeddings, and is pretrained using MLM.

SimSon (Lee et al. 2025) uses an encoder-only backbone and is pretrained by contrastive SSL. Randomized SMILES strings of the same molecule form positive pairs, while strings from different molecules form negative pairs. Despite using such a simple pretraining procedure and a much smaller dataset, SimSon is shown to be competitive with the aforementioned architectures.

ChemFM (Cai et al. 2024) is built on an encoder-only LLaMA (Touvron et al. 2023) backbone and is pretrained using GPT-style causal language modeling (CLM). It is significantly larger than other models, with 1B and 3B parameter variants. The molecule embedding is derived from the output vector of the end-of-sequence ([EOS]) token.

ChemGPT (Frey et al. 2023) adopts a decoder-only architecture based on GPT-Neo (Black et al. 2021), and is trained on SELFIES strings using CLM. The authors train multiple model variants up to 1.3B parameters, demonstrating that neural scaling laws hold for chemistry-focused text-based transformers as well.

SELMFormer (Yüksel et al. 2023) is based on an encoder-only RoBERTa architecture but uses SELFIES, rather than SMILES. Its authors assume that the more regular syntax of SELFIES facilitates learning and improves the capture of relevant molecular patterns. Pretraining uses the MLM objective.

Hybrid models

Mol2Vec (Jaeger, Fulle, and Turk 2018) combines graph-based ECFP4 descriptors with the text-based Word2Vec approach (Mikolov et al. 2013) to learn context-aware token representations. It first computes integer ECFP identifiers for circular subgraphs centered on each atom, using radii 0 and 1. These subgraphs are treated as words in a sequence, with each one forming a token. A Word2Vec skip-gram model is then used to pretrain context-aware vector representations for each token. During inference, all subgraph vectors are summed to obtain a whole-molecule embedding.

COATI (Kaufman et al. 2024) employs a multimodal encoder-decoder architecture, pretrained using CLIP-style (Radford et al. 2021) multimodal contrastive learning. The 3D molecule conformer is encoded using an E(3)-equivariant GNN (Satorras, Hoogeboom, and Welling 2021), and its SMILES string with a RoFormer (Su et al. 2024). The model is pretrained with two objectives: contrastive learning between those two representations (treating embeddings of the same molecule as positive pairs), and autoregressive SMILES reconstruction using a decoder. At inference time, molecular embeddings are obtained from the SMILES encoder.

CLAMP (Seidl et al. 2023) is a multimodal encoder model trained with supervised contrastive learning based on ChEMBL bioactivity assay data. Each molecule is encoded via the concatenation of three molecular fingerprints (ECFP, RDKit, and MACCS) processed through a two-layer MLP, which serves as the final embedding. Assay descriptions are encoded using Latent Dirichlet Allocation (LDA). Positive pairs consist of a bioactive molecule and the description of the assay in which it is active, while negative pairs involve nonbioactive compounds. This design incorporates a bioactivity-specific inductive bias into the fingerprint-based representation.

Methods

We comprehensively evaluated molecular embeddings using 25 datasets - 7 from MoleculeNet (Wu et al. 2018) and 18 from TDC (Huang et al. 2021) - as they are among the most widely used benchmarks in molecular property prediction. Our focus is on classification tasks, as it is the most common approach in virtual screening (binary bioactivity classification) and ADMET prediction. Regression models were also very unstable in the initial experiments. The datasets span a broad range of tasks, including ADME, various toxicity endpoints, virtual screening, and more. In particular, TDC datasets include several small ones that reflect real-world ML-assisted drug discovery scenarios, where fine-tuning results in catastrophic overfitting. For a realistic out-of-distribution evaluation, we use a challenging scaffold-based train-test splits.

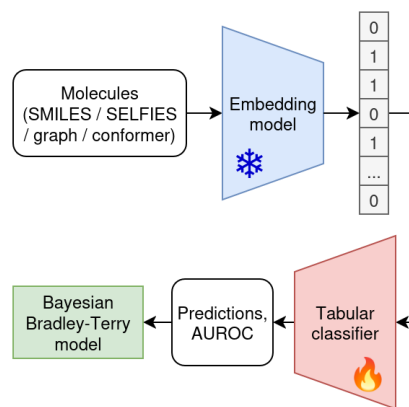


Figure 1: The proposed workflow.

All 25 models described in the Molecular Embedding Approaches section were evaluated. For models with multiple variants (e.g. different neural network sizes), all were implemented, and the best-performing variant (based on average AUROC) was selected. We extracted frozen embeddings (without fine-tuning) and trained the same classification models on top of these features. This setup, inspired by approaches like DINO in computer vision, ensures a fair comparison by removing confounding factors such as downstream classifier architecture, parameter count, or finetuning strategy. Only the pretrained model’s knowledge and its transferability affect performance. For classification, we used Random Forest (RF), logistic regression (LR), and k-nearest neighbors (kNN). RF and LR are widely used in chemoinformatics because of their strong performance on small datasets. kNN, being instance-based and parameter-free, isolates performance differences to the quality of the embeddings. The hyperparameter tuning was identical across all datasets and models to ensure fairness.

We used the area under the receiver operating characteristic curve (AUROC) as an evaluation metric. AUROC is well-suited for imbalanced datasets, common in molecular ML, and is widely adopted in chemoinformatics, including in MoleculeNet and TDC benchmarks. The ECFP count fingerprint was used as the main baseline, due to its popularity, strong theoretical foundations, and consistently strong practical performance (Rogers and Hahn 2010). It also captures more information than its binary variant (Adamczyk and Ludyndia 2024).

The benchmarking problem addressed in this work can be framed as a comparison of multiple models on multiple datasets (Demšar 2006). Bayesian testing is recommended for this setting (Benavoli et al. 2017), offering advantages over frequentist methods such as higher statistical power, interpretable posterior distributions, and the ability to define a region of practical equivalence (ROPE). Specifically, we use the hierarchical Bayesian Bradley-Terry (BBT) model (Wainer 2023), which is designed for multimodel comparisons. It provides clear decisions on whether one model outperforms another, is practically equivalent, or if the evidence

is inconclusive, while offering strong theoretical grounding and intuitive probabilistic interpretation. We follow the recommendations of (Wainer 2023) for model interpretation, but expand the ROPE to 25–75%. That is, if the probability that one model outperforms another in a given dataset falls within $[0.25, 0.75]$, we consider them practically equivalent. This makes the comparisons more conservative, reducing false positives when evaluating many models. Despite this much stricter criterion, the BBT model still yields very confident rankings, as detailed in the Results section.

Figure 1 illustrates our approach. This setup enables the rigorous evaluation of numerous models on a large-scale, diverse benchmark under a fair comparison framework, with analysis conducted using the dedicated BBT model. See the Supplementary Material for details on datasets, model variants, hyperparameter grids, hardware, and further explanation of Bayesian tests and the BBT model.

Results

The aggregated results of the model, the average rank, and the AUROC, are shown in Table 1. The key finding is that only four models outperformed the ECFP fingerprint. The top-performing model, CLAMP, is a fusion of molecular fingerprints. The other three - R-MAT, MolBERT, and ChemBERTa - use distinct architectures and pretraining strategies. We note that the MTR variant, incorporating more chemistry-specific knowledge into pretraining, vastly outperformed the MLM variant in all cases (see the Supplementary Material for details), and thus it is also used here.

Among the worst-performing models, most are based on message-passing GNNs, with the best of them, MolR, achieving an average rank of 13.84. SELFIES-based text transformers also ranked among the weakest performers.

Bayesian testing

Aggregated metrics alone, such as mean AUROC and mean rank, are insufficient for a fair comparison of the models (Demšar 2006; Wainer 2023). Mean AUROC is sensitive to outliers (e.g., datasets unusually easy for certain models), while mean rank ignores the magnitude of performance differences. To address these limitations, we use the BBT model, designed specifically for robust multi-model comparisons. The results, with ECFP as the baseline, are shown in Table 2. Following the procedure described in (Wainer 2023), we categorize models as: better than ECFP, equivalent (within the ROPE), worse or undecidable (insufficient evidence). All posterior probabilities are provided in the Supplementary Material.

These results show that only the CLAMP model is statistically significantly better than ECFP. Further analyses in the following sections confirm that CLAMP is the only model that consistently outperforms, or at least matches, other approaches.

ChemBERTa is practically equivalent to ECFP, but comes with significantly higher computational and memory costs. For CDDD, the evidence is inconclusive, meaning it performs much better or worse than ECFP depending on the dataset. A key practical advantage of hierarchical Bayesian

Model	Mean rank ↓	Mean AUROC ↑
CLAMP	5.40	82.55%
R-MAT	6.08	80.83%
MolBERT	6.92	80.51%
ChemBERTa	7.32	79.99%
ECFP	7.52	79.89%
CDDD	7.64	80.60%
Atom Pair	7.88	79.48%
MAT	8.02	80.18%
MolFormer	9.50	79.80%
Mol2Vec	10.36	79.55%
TT	12.04	78.12%
ChemFM	12.60	78.25%
Uni-Mol2	13.32	78.11%
MolR	13.80	77.84%
COATI	13.92	78.02%
GraphMVP	14.64	77.18%
Chemformer	15.00	77.44%
Uni-Mol	16.64	76.85%
GROVER	17.08	75.68%
GIN	17.28	75.14%
SimSon	19.12	73.56%
ChemGPT	19.32	74.01%
GEM	19.36	74.03%
SELFormer	20.04	73.18%
GraphFP	24.20	59.67%

Table 1: Average model results.

BBT decision	Models
Better	CLAMP
Practically equivalent	ChemBERTa
No decision can be made	CDDD
Worse	R-MAT, MolBERT, ..., (all other models)

Table 2: Bayesian Bradley-Terry (BBT) model decisions, comparing pretrained models to the ECFP baseline.

testing is its ability to capture such nuanced relationships while accounting for multiple hypothesis testing, something that traditional null hypothesis testing cannot do (Benavoli et al. 2017).

Despite having a higher average rank and AUROC, R-MAT and MolBERT are deemed worse than ECFP by the BBT model, suggesting that their apparent performance may be driven by outliers on just a few datasets. R-MAT was closer to equivalence, with a probability 80% of falling within ROPE. All other models, including AP and TT molecular fingerprints, are significantly worse than ECFP. This does not mean that these models always perform poorly, but that their overall likelihood of outperforming ECFP is low. Such insights help guide model selection, reducing engineering effort and computational cost.

We also note that we used a conservative ROPE range of

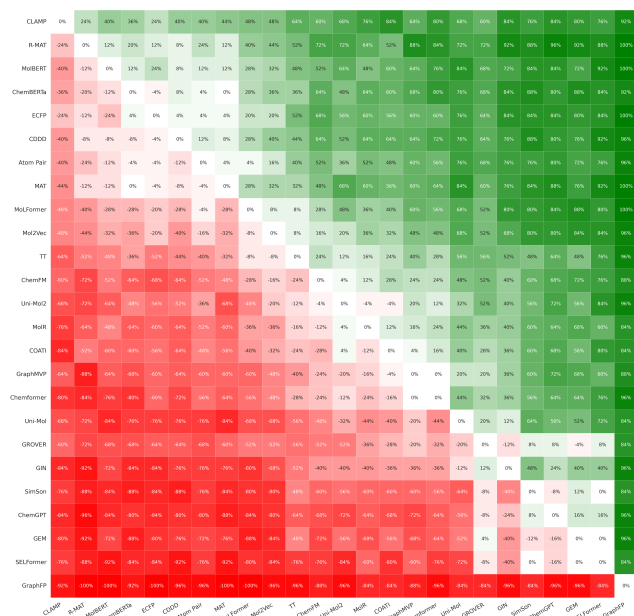


Figure 2: Pairwise win ratio between all evaluated models. Green marks wins of model on Y axis against model on X axis, red means losses (i.e., model from X axis won more).

25-75%. Despite this wide interval, the BBT model remains very confident in its conclusions, often assigning a probability near 100%. The detailed tables are available in the Supplementary Material.

Inter-model win rates

Figure 2 provides a detailed analysis of win rates between models, showing the percentage of datasets where one model outperforms another. Models are ranked by their number of wins against the ECFP baseline. To exclude insignificant differences, following (Benavoli et al. 2017), we treat AUROC differences below 0.01% as ties (practical equivalence). We also apply this for all subsequent analyses.

The results align with the Bayesian analysis. Notably, CLAMP consistently wins or ties against all other models, which is impressive given the diversity of datasets in terms of ADMET endpoints. In contrast, GraphFP performs worst despite its strong graph and chemistry-based inductive biases. SELFIES-based models also show underwhelming results.

Per-dataset wins against ECFP

Figure 3 shows the percentage of models that outperform the ECFP baseline on each dataset. Notably, on 5 datasets no model outperforms ECFP, and on 8 more, only one or two models do. This highlights the importance of rigorous benchmarking, even against well-established models, to fairly evaluate new algorithms.

We also counted how many datasets each model won or tied for a win. Table 3 summarizes models with at least five wins or near-wins (see the Supplementary Material for full details). Again, only CLAMP, a molecular fingerprint-based

Model	Number of datasets
CLAMP	14
Atom Pair	7
R-MAT	6
ChemBERTa	5
ECFP	5

Table 3: The number of datasets, where a given model won or had a near-win.

model, consistently performs well, winning or nearly winning on 14 datasets, more than half the benchmark.

Discussion and practical remarks

Overall, our experiments consistently show that pretrained molecular embedding models based on various neural networks often fail to outperform the ECFP baseline, as well as the Atom Pair and Topological Torsion fingerprints. This suggests that progress in molecular representation learning, when properly evaluated, is less substantial than commonly claimed.

In fact, only the CLAMP model performs consistently well. It relies on a smart fusion of molecular fingerprints combined with a shallow MLP for pretraining, underscoring that well-designed, domain-specific feature extraction methods still provide competitive performance in practical cheminformatics.

Other well-performing models are almost exclusively transformers that incorporate strong molecular-specific biases, such as molecular attention in R-MAT and MAT, or property prediction tasks in MolBERT and ChemBERTa’s MTR pretraining. This highlights an important lesson for future development: relying solely on large pretraining datasets and generic graph- or NLP-based architectures is insufficient for chemical data. Domain-specific knowledge and tailored model modifications are essential.

Qualitatively, reproducibility and code quality strongly correlated with model performance. The best models featured easy-to-run, well-documented code and dependencies. Molecular fingerprint baselines implemented with `scikit-fingerprints` (Adamczyk and Ludynia 2024) were also very user-friendly. In contrast, models requiring substantial engineering effort to run, such as GraphFP, GEM, or GraphMVP, often delivered disappointing results.

Finally, we offer practical recommendations for practitioners in molecular representation learning and cheminformatics:

1. Always include the ECFP count fingerprint as a baseline, paired with a tree-based classifier. Ideally, test other fingerprints like Atom Pair.
2. Consider the CLAMP model, especially when using embeddings without fine-tuning neural networks (e.g., with very small datasets).
3. Other notable models to try are R-MAT, MolBERT, ChemBERTa, and CDDD. These are relatively easy to set up, but may show variable performance and often underperform compared to ECFP.

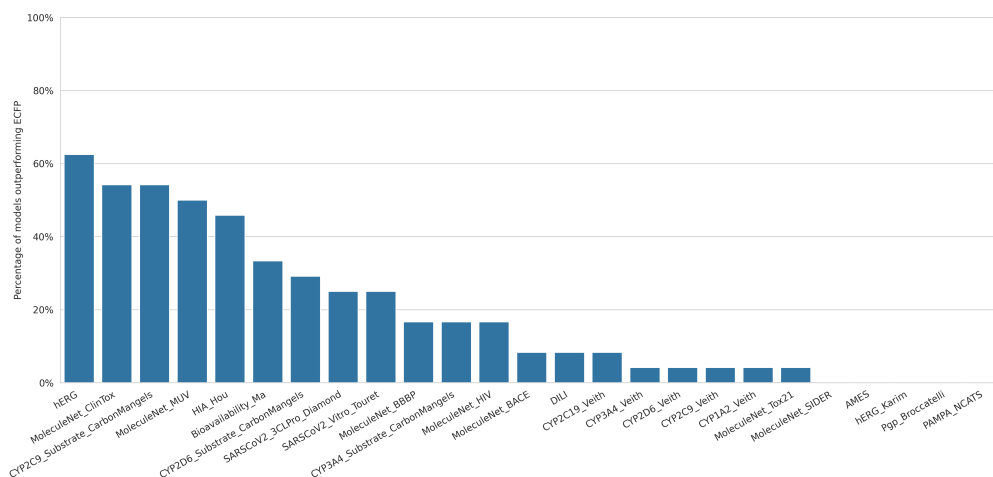


Figure 3: Percentage of models outperforming ECFP for each dataset.

- Avoid models that tend to perform poorly and require significant effort to run, such as GraphFP, GEM, and GraphMVP (see Table 1 and Figure 2). Use them only if substantial engineering and computational resources are available.
- We echo existing literature (Benavoli et al. 2017; Wainer 2023) recommending Bayesian statistical tests, particularly the Bayesian Bradley-Terry (BBT) model, for multi-model, multi-dataset comparisons, as they provide clear aggregation and intuitive interpretation of results.

Conclusions

We presented a comprehensive benchmark of pretrained molecular representation models. Analysis of 25 models on 25 datasets, based on a fair comparison setting and supported with a Bayesian Bradley-Terry model, challenges perceived progress in this domain and indicates inadequate evaluation rigor in previous works. All models, except CLAMP, are either worse than or practically equivalent to the baseline ECFP fingerprint on molecular property prediction tasks. Furthermore, the representations learned by GNNs are of significantly worse quality than those of other approaches, including molecular fingerprints. Those findings call for further in-depth empirical and theoretical analyses, to increase the practical relevance of ML models for drug development and chemoinformatics.

References

Adamczyk, J.; and Czech, W. 2023. Strengthening structural baselines for graph classification using Local Topological Profile. In *International Conference on Computational Science*, 597–611. Springer.

Adamczyk, J.; and Czech, W. 2024. Molecular Topological Profile (MOLTOP)-Simple and Strong Baseline for Molecular Graph Classification. In *ECAI 2024*, 1575–1582. IOS Press.

Adamczyk, J.; and Ludynia, P. 2024. Scikit-fingerprints:

Easy and efficient computation of molecular fingerprints in Python. *SoftwareX*, 28: 101944.

Adamczyk, J.; Ludynia, P.; and Czech, W. 2025. Molecular Fingerprints Are Strong Models for Peptide Function Prediction. *arXiv preprint arXiv:2501.17901*.

Baptista, D.; Correia, J.; Pereira, B.; and Rocha, M. 2022. Evaluating molecular representations in machine learning models for drug response prediction and interpretability. *Journal of Integrative Bioinformatics*, 19(3): 20220006.

Benavoli, A.; Corani, G.; Demšar, J.; and Zaffalon, M. 2017. Time for a Change: a Tutorial for Comparing Multiple Classifiers Through Bayesian Analysis. *Journal of Machine Learning Research*, 18(77): 1–36.

Black, S.; Gao, L.; Wang, P.; Leahy, C.; and Biderman, S. 2021. GPT-Neo: Large Scale Autoregressive Language Modeling with Mesh-Tensorflow.

Cai, F.; Hanna, K.; Zhu, T.; Tzeng, T.-R.; Duan, Y.; Liu, L.; Pilla, S.; Li, G.; and Luo, F. 2024. A Foundation Model for Chemical Design and Property Prediction. *arXiv preprint arXiv:2410.21422*.

Caron, M.; Touvron, H.; Misra, I.; Jégou, H.; Mairal, J.; Bojanowski, P.; and Joulin, A. 2021. Emerging Properties in Self-Supervised Vision Transformers. In *Proceedings of the IEEE/CVF International Conference on Computer Vision*, 9650–9660. Introduces DINO.

Chithrananda, S.; Grand, G.; and Ramsundar, B. 2020. ChemBERTa: Large-Scale Self-Supervised Pretraining for Molecular Property Prediction. In *MLA Molecules - NeurIPS 2020 Workshop*.

Demšar, J. 2006. Statistical Comparisons of Classifiers over Multiple Data Sets. *Journal of Machine Learning Research*, 7(Jan): 1–30.

Du, J.; Zhang, S.; Wu, G.; Moura, J. M.; and Kar, S. 2017. Topology Adaptive Graph Convolutional Networks. *arXiv preprint arXiv:1710.10370*.

Fabian, B.; Edlich, T.; Gaspar, H.; Segler, M.; Meyers, J.; Fiscato, M.; and Ahmed, M. 2020. Molecular representation

- learning with language models and domain-relevant auxiliary tasks. In *ML4Molecules - NeurIPS 2020 Workshop*.
- Fang, X.; Liu, L.; Lei, J.; He, D.; Zhang, S.; Zhou, J.; Wang, F.; Wu, H.; and Wang, H. 2022. Geometry-enhanced molecular representation learning for property prediction. *Nature Machine Intelligence*, 4(2): 127–134.
- Frey, N. C.; Soklaski, R.; Axelrod, S.; Samsi, S.; Gomez-Bombarelli, R.; Coley, C. W.; and Gadepally, V. 2023. Neural scaling of deep chemical models. *Nature Machine Intelligence*, 5(11): 1297–1305.
- Gilmer, J.; Schoenholz, S. S.; Riley, P. F.; Vinyals, O.; and Dahl, G. E. 2017. Neural Message Passing for Quantum Chemistry. In *International Conference on Machine Learning*, 1263–1272. Pmlr.
- Hu, W.; Liu, B.; Gomes, J.; Zitnik, M.; Liang, P.; Pande, V.; and Leskovec, J. 2020. Strategies for Pre-training Graph Neural Networks. In *International Conference on Learning Representations*.
- Huang, K.; Fu, T.; Gao, W.; Zhao, Y.; Roohani, Y. H.; Leskovec, J.; Coley, C. W.; Xiao, C.; Sun, J.; and Zitnik, M. 2021. Therapeutics Data Commons: Machine Learning Datasets and Tasks for Drug Discovery and Development. In *Thirty-fifth Conference on Neural Information Processing Systems Datasets and Benchmarks Track (Round 1)*.
- Irwin, R.; Dimitriadis, S.; He, J.; and Bjerrum, E. J. 2022. Chemformer: a pre-trained transformer for computational chemistry. *Machine Learning: Science and Technology*, 3(1): 015022.
- Jaeger, S.; Fulle, S.; and Turk, S. 2018. Mol2vec: Unsupervised Machine Learning Approach with Chemical Intuition. *Journal of Chemical Information and Modeling*, 58(1): 27–35.
- Ji, X.; Wang, Z.; Gao, Z.; Zheng, H.; Zhang, L.; Ke, G.; and E, W. 2024. Exploring Molecular Pretraining Model at Scale. In *The Thirty-eighth Annual Conference on Neural Information Processing Systems*.
- Jiang, D.; Wu, Z.; Hsieh, C.-Y.; Chen, G.; Liao, B.; Wang, Z.; Shen, C.; Cao, D.; Wu, J.; and Hou, T. 2021. Could graph neural networks learn better molecular representation for drug discovery? A comparison study of descriptor-based and graph-based models. *Journal of Cheminformatics*, 13(1): 12.
- Kaufman, B.; Williams, E. C.; Underkoffler, C.; Pederson, R.; Mardirossian, N.; Watson, I.; and Parkhill, J. 2024. COATI: Multimodal Contrastive Pretraining for Representing and Traversing Chemical Space. *Journal of Chemical Information and Modeling*, 64(4): 1145–1157.
- Krenn, M.; Häse, F.; Nigam, A.; Friederich, P.; and Aspuru-Guzik, A. 2020. Self-referencing embedded strings (SELF-IES): A 100% robust molecular string representation. *Machine Learning: Science and Technology*, 1(4): 045024.
- Landrum, G.; Tosco, P.; Kelley, B.; Rodriguez, R.; Cosgrove, D.; Vianello, R.; sriniker; Gedeck, P.; Jones, G.; Kawashima, E.; NadineSchneider; Nealschneider, D.; Dalke, A.; Swain, M.; Cole, B.; tadhurst-cdd; Turk, S.; Savelev, A.; Vaucher, A.; Wójcikowski, M.; Take, I.; Walker, R.; Scalfani, V. F.; Faara, H.; Ujihara, K.; Probst, D.; Maeder, N.; Monat, J.; Lehtivarjo, J.; and Godin, G. 2025. RDKit: Open-source Cheminformatics. <https://www.rdkit.org>.
- Lee, C. E.; Kim, J. S.; Min, J. H.; and Han, S. W. 2025. SimSon: simple contrastive learning of SMILES for molecular property prediction. *Bioinformatics*, 41(5): btaf275.
- Lewis, M.; Liu, Y.; Goyal, N.; Ghazvininejad, M.; Mohamed, A.; Levy, O.; Stoyanov, V.; and Zettlemoyer, L. 2020. BART: Denoising Sequence-to-Sequence Pre-training for Natural Language Generation, Translation, and Comprehension. In Jurafsky, D.; Chai, J.; Schluter, N.; and Tetreault, J., eds., *Proceedings of the 58th Annual Meeting of the Association for Computational Linguistics*, 7871–7880. Online: Association for Computational Linguistics.
- Liu, S.; Wang, H.; Liu, W.; Lasenby, J.; Guo, H.; and Tang, J. 2022. Pre-training Molecular Graph Representation with 3D Geometry. In *International Conference on Learning Representations*.
- Luong, K.-D.; and Singh, A. K. 2023. Fragment-based Pre-training and Finetuning on Molecular Graphs. *Advances in Neural Information Processing Systems*, 36: 17584–17601.
- Maziarka, Ł.; Danel, T.; Mucha, S.; Rataj, K.; Tabor, J.; and Jastrzębski, S. 2020. Molecule Attention Transformer. *arXiv preprint arXiv:2002.08264*.
- Maziarka, Ł.; Majchrowski, D.; Danel, T.; Gaiński, P.; Tabor, J.; Podolak, I.; Morkisz, P.; and Jastrzębski, S. 2024. Relative molecule self-attention transformer. *Journal of Cheminformatics*, 16(1): 3.
- Mikolov, T.; Chen, K.; Corrado, G.; and Dean, J. 2013. Efficient Estimation of Word Representations in Vector Space. *arXiv preprint arXiv:1301.3781*.
- Nilakantan, R.; Bauman, N.; Dixon, J. S.; and Venkataraghavan, R. 1987. Topological torsion: a new molecular descriptor for SAR applications. Comparison with other descriptors. *Journal of Chemical Information and Computer Sciences*, 27(2): 82–85.
- Radford, A.; Kim, J. W.; Hallacy, C.; Ramesh, A.; Goh, G.; Agarwal, S.; Sastry, G.; Askell, A.; Mishkin, P.; Clark, J.; et al. 2021. Learning Transferable Visual Models From Natural Language Supervision. In *International Conference on Machine Learning*, 8748–8763. Pmlr.
- Rogers, D.; and Hahn, M. 2010. Extended-connectivity fingerprints. *Journal of Chemical Information and Modeling*, 50(5): 742–754.
- Rong, Y.; Bian, Y.; Xu, T.; Xie, W.; Wei, Y.; Huang, W.; and Huang, J. 2020. Self-Supervised Graph Transformer on Large-Scale Molecular Data. *Advances in Neural Information Processing Systems*, 33: 12559–12571.
- Ross, J.; Belgodere, B.; Chenthamarakshan, V.; Padhi, I.; Mroueh, Y.; and Das, P. 2022. Large-scale chemical language representations capture molecular structure and properties. *Nature Machine Intelligence*, 4(12): 1256–1264.
- Satorras, V. G.; Hoogeboom, E.; and Welling, M. 2021. E(n) Equivariant Graph Neural Networks. In *International Conference on Machine Learning*, 9323–9332. PMLR.

Schütt, K. T.; Saucedo, H. E.; Kindermans, P.-J.; Tkatchenko, A.; and Müller, K.-R. 2018. SchNet - a deep learning architecture for molecules and materials. *The Journal of Chemical Physics*, 148(24).

Seidl, P.; Vall, A.; Hochreiter, S.; and Klambauer, G. 2023. Enhancing Activity Prediction Models in Drug Discovery with the Ability to Understand Human Language. In *International Conference on Machine Learning*, 30458–30490. PMLR.

Su, J.; Ahmed, M.; Lu, Y.; Pan, S.; Bo, W.; and Liu, Y. 2024. RoFormer: Enhanced Transformer with Rotary Position Embedding. *Neurocomputing*, 568: 127063.

Touvron, H.; Lavril, T.; Izacard, G.; Martinet, X.; Lachaux, M.-A.; Lacroix, T.; Rozière, B.; Goyal, N.; Hambro, E.; Azhar, F.; et al. 2023. LLaMA: Open and Efficient Foundation Language Models. *arXiv preprint arXiv:2302.13971*.

Wainer, J. 2023. A Bayesian Bradley-Terry model to compare multiple ML algorithms on multiple data sets. *Journal of Machine Learning Research*, 24(341): 1–34.

Wang, H.; Li, W.; Jin, X.; Cho, K.; Ji, H.; Han, J.; and Burke, M. D. 2022. Chemical-Reaction-Aware Molecule Representation Learning. In *International Conference on Learning Representations*.

Wang, K.; Reimers, N.; and Gurevych, I. 2021. TS-DAE: Using Transformer-based Sequential Denoising Auto-Encoder for Unsupervised Sentence Embedding Learning. In *Findings of the Association for Computational Linguistics: EMNLP 2021*, 671–688. Introduces the TS-DAE training objective.

Weininger, D. 1988. SMILES, a chemical language and information system. 1. Introduction to methodology and encoding rules. *Journal of Chemical Information and Computer Sciences*, 28(1): 31–36.

Winter, R.; Montanari, F.; Noé, F.; and Clevert, D.-A. 2019. Learning continuous and data-driven molecular descriptors by translating equivalent chemical representations. *Chemical Science*, 10(6): 1692–1701.

Wu, Z.; Ramsundar, B.; Feinberg, E. N.; Gomes, J.; Geniesse, C.; Pappu, A. S.; Leswing, K.; and Pande, V. 2018. MoleculeNet: a benchmark for molecular machine learning. *Chemical Science*, 9(2): 513–530.

Xu, K.; Hu, W.; Leskovec, J.; and Jegelka, S. 2019. How Powerful are Graph Neural Networks? In *International Conference on Learning Representations*.

Yüksel, A.; Ulusoy, E.; Ünlü, A.; and Doğan, T. 2023. SELFormer: Molecular Representation Learning via SELFIES Language Models. *Machine Learning: Science and Technology*, 4(2): 025035.

Zhou, G.; Gao, Z.; Ding, Q.; Zheng, H.; Xu, H.; Wei, Z.; Zhang, L.; and Ke, G. 2023. Uni-Mol: A Universal 3D Molecular Representation Learning Framework. In *The Eleventh International Conference on Learning Representations*.

Supplementary Material

Datasets

Table 4 summarizes all datasets used in this study, reporting general statistics including the number of molecules, number of tasks, and the mean proportion of positive samples. A small subset of molecules (less than 0.01%) from the MoleculeNet_HIV dataset was excluded due to parsing errors encountered with the SELFIES translator. In addition, a very small fraction of molecules (less than 0.003%) containing dative bonds was removed, as these structures caused errors in certain models.

Model variants

We tried to incorporate all of the subvariants available from open-weight pre-trained models available. Below we present the list of all of the models for each of the architectures:

- CDDD;
- CLAMP;
- ChemBERTa – 5M, 10M, 77M (meaning the size of pre-training dataset), with MTR and MLM pretraining;
- ChemFM – 1B and 3B parameters;
- ChemGPT – 4.7M and 19M parameters;
- GEM;
- ContextPred – based on GraphMVP code
- GraphFP – C and CP variants;
- GraphMVP – contrastive and generative model, with two variants of SSL loss, Attribute Masking and Context Prediction, and 3 pooling variants: mean, sum, max, resulting in 6 variants overall;
- MolFormer;
- SELFormer and SELFormer Lite;
- SimSon;
- Chemformer – augment, mask and combined;
- COATI;
- GROVER – base and large;
- MAT – 200k, 2M and 20M parameters;
- Mol2Vec;
- MolR – GCN, GAT, SAGE, and TAG variants;
- MolBERT;
- R-MAT 4M;
- Uni-Mol;
- Uni-Mol2.

Classifiers and hyperparameter tuning

Three classifiers were implemented on top of embeddings: Random Forest, logistic regression, and k nearest neighbors. All underwent hyperparameter tuning, exactly the same on all datasets, with the exception of the largest MUV dataset. In that case, kNN didn’t finish in reasonable time (24 hours on an HPC server) for any model, so we omit this combination. For results in the main body, for each dataset and embedder we select the best model of the three.

Hyperparameter grids were designed to result in reasonable computational time, and also give good results based on initial experiments. For Random Forest, we tune `min_samples_split` in range [2, 4, 6, 8, 10, and always use 500 trees with entropy loss function, following e.g. Local Topological Profile (Adamczyk and Czech 2023) and MOLTOP (Adamczyk and Czech 2024). For logistic regression, we tune reverse regularization strength λ , as 10 values on logarithmic scale from 10^{-2} to 10^3 . For kNN, we tune number of neighbors k in range [1, 3, 5, 7, 9].

Hardware used

The experiments were conducted on a server running Linux kernel version 6.1.115, equipped with an AMD EPYC 7763 processor (64 cores, 2.45 GHz) and 512 GB of RAM. For models supporting GPU acceleration, an NVIDIA RTX A4000 GPU was utilized.

Bayesian statistical tests

We compare many pretrained molecular embedding models across many datasets using a hierarchical Bayesian Bradley–Terry (BBT) model. The BBT treats per-dataset pairwise outcomes (“model i beats model j ” vs “model j beats i ”) as binomial observations whose success probability is a logistic function of latent model “abilities”, and then infers the posterior distribution of all pairwise win probabilities. This delivers (i) a single aggregated ranking, (ii) calibrated posterior probabilities that one model outperforms another on a new dataset, and (iii) a principled way to declare practical equivalence through a region of practical equivalence (ROPE) defined directly in probability space.

Data preparation

For every model and every classification dataset, we compute AUROC using a fixed training-test split (scaffold split) and a common downstream classifier head (RF, LR, or kNN) trained on frozen embeddings, to isolate representation quality. As Bayesian tests require the same metric to be used everywhere, AUROC is used uniformly across tasks due to its robustness to class imbalance.

Within each dataset, we compare all model pairs. If the AUROC difference is smaller than a prespecified metric-level practical equivalence threshold, we record a tie for that

Dataset	Benchmark	No. samples	No. tasks	Mean share of positive samples
AMES	TDC	7278	1	54.60%
Bioavailability_Ma	TDC	640	1	76.88%
CYP1A2_Veith	TDC	12579	1	46.34%
CYP2C19_Veith	TDC	12665	1	45.95%
CYP2C9_Substrate_CarbonMangels	TDC	669	1	21.08%
CYP2C9_Veith	TDC	12092	1	33.45%
CYP2D6_Substrate_CarbonMangels	TDC	667	1	28.64%
CYP2D6_Veith	TDC	13130	1	19.15%
CYP3A4_Substrate_CarbonMangels	TDC	670	1	52.99%
CYP3A4_Veith	TDC	12328	1	41.45%
DILI	TDC	475	1	49.68%
HIA_Hou	TDC	578	1	86.51%
PAMPA_NCATS	TDC	2034	1	85.50%
Pgp_Broccatelli	TDC	1218	1	53.37%
SARSCoV2_3CLPro_Diamond	TDC	880	1	8.86%
SARSCoV2_Vitro_Touret	TDC	1484	1	5.93%
hERG	TDC	655	1	68.85%
hERG_Karim	TDC	13445	1	49.97%
MoleculeNet_BACE	MoleculeNet	1513	1	45.67%
MoleculeNet_BBBP	MoleculeNet	2039	1	76.51%
MoleculeNet_ClinTox	MoleculeNet	1477	2	50.61%
MoleculeNet_HIV	MoleculeNet	41084	1	3.50%
MoleculeNet_MUV	MoleculeNet	93087	17	0.20%
MoleculeNet_SIDER	MoleculeNet	1427	27	56.76%
MoleculeNet_Toxt21	MoleculeNet	7831	12	7.52%

Table 4: List of datasets used in the evaluation along with the general statistic in form of the number of samples, number of tasks and mean share of positive samples.

dataset; otherwise, the higher-AUROC model records a win on that dataset. In our experiments we treated AUROC differences below 0.01% as ties, following the “practical equivalence” spirit advocated in Bayesian testing for ML comparisons. This prevents trivial numerical differences from counting as wins.

Bayesian Bradley–Terry model

Bayesian procedures return the posterior probability that one model is better than another and allow explicit probability statements about practical equivalence, overcoming well-known limitations of frequentist NHST in this setting, e.g., p-values confound effect size and sample size; non-significance does not imply equivalence (Benavoli et al. 2017). Let $P(i \succ j)$ be a Bayesian posterior-predictive probability: “the probability that model i beats model j ”. $P(i \succ j)$ is the central quantity reported by the Bayesian Bradley–Terry model (Wainer 2023): it combines the empirical evidence (observed wins), model assumptions (the logistic link), and parameter uncertainty into a single, decision-relevant probability.

Pairwise win counts For every ordered pair of models (i, j) let W_{ij} be the (possibly fractional)¹ number of datasets on which model i outperforms model j . We denote the total

¹Ties are handled by the “spread” rule; each tie contributes 0.5 to both W_{ij} and W_{ji} .

number of comparisons by:

$$N_{ij} = W_{ij} + W_{ji}.$$

Likelihood The win counts are modeled with a binomial Bradley–Terry likelihood:

$$W_{ij} \sim \text{Binomial}(N_{ij}, \pi_{ij}), \quad (1)$$

$$\pi_{ij} = \frac{\exp(\beta_i)}{\exp(\beta_i) + \exp(\beta_j)} = (1 + e^{-(\beta_i - \beta_j)})^{-1} \quad (2)$$

Priors Latent abilities β_i are given a hierarchical Gaussian prior with shared scale σ :

$$\beta_i \sim \mathcal{N}(0, \sigma^2), \quad (3)$$

$$\sigma \sim \text{LogNormal}(0, 0.5^2), \quad (4)$$

$$\sum_{i=1}^M \beta_i = 0 \quad (\text{identifiability}). \quad (5)$$

Posterior inference We sample from the joint posterior $p(\beta, \sigma \mid \{W_{ij}\})$ by Markov-Chain Monte Carlo (Stan implementation). Convergence is checked, and posterior predictive checks (PPCs) are used to confirm that the observed win counts are plausible draws from the fitted model.

Posterior summaries For each ordered pair (i, j) and each MCMC draw s ,

$$\pi_{ij}^{(s)} = \text{logit}^{-1}(\beta_i^{(s)} - \beta_j^{(s)}).$$

we report: (i) the posterior mean $\hat{\pi}_{ij}$, (ii) the 89% highest-density interval (HDI), (iii) $P_{\text{in ROPE}}$, the posterior mass lying inside the prespecified probability ROPE $[\rho_L, \rho_U]$, (iv) $P_{\text{above } 0.5}$, the probability that model i truly outperforms model j . Global abilities are summarised by the posterior means $\hat{\beta}_i = \mathbb{E}[\beta_i]$, which induce a unique ranking, while retaining full pairwise uncertainty.

Decision rule Let $[\rho_L, \rho_U] = [0.25, 0.75]$ be the probability-space region of practical equivalence (ROPE):

- declare i better than $j \iff \hat{\pi}_{ij} > \rho_U$,
- declare equivalence $\iff P_{\text{in ROPE}} \geq 0.95$.

Pairs that satisfy neither condition are deemed inconclusive.

Aggregated ranking We order models by the posterior mean of β_i . This yields a unique global ranking while retaining pairwise posteriors for uncertainty-aware claims.

Decision rules and ROPE

The BBT supports a universal probability ROPE, independent of the downstream metric’s scale. Wainer proposes $[0.45, 0.55]$: if the posterior lies largely in $[0.45, 0.55]$ models i and j are practically equivalent. Researchers may widen or narrow this interval depending on conservativeness. Following Wainer’s guidance for interpretation but opting for stronger conservativeness when many models are compared, we used a wide probability ROPE of $[0.25, 0.75]$. Despite this strict criterion, posterior probabilities were often near 1.0 or 0.0, yielding confident decisions.

Step-by-step protocol

1. **Compute per-dataset scores:** For each dataset and model, compute AUROC under the shared evaluation protocol (frozen embeddings + fixed classifier head).
2. **Within-dataset pairwise comparisons:** For each data set and each pair of models (i, j) : if $|AUROC_i - AUROC_j| < \epsilon$ ($\epsilon = 0.01$, i.e. 1%) record a tie; else, record a win for the higher AUROC model.
3. **Build the win/loss table:** Sum wins across datasets for every ordered pair (i, j) convert ties with the spread policy (each tie contributes 0.5 to both sides).
4. **Fit the BBT:** Use the binomial/logistic likelihood with hierarchical priors $\beta_i \sim \mathcal{N}(0, \sigma^2)$, $\sigma \sim \text{LogNorm}(0, 0.5^2)$; sample via MCMC to obtain posterior draws of $\{\beta_i\}$. Check convergence and perform PPC.
5. **Summarize pairwise posteriors:** For every pair: (i, j) transform draws of $\beta_i - \beta_j$ to draws of $P(i \succ j)$, report the posterior mean, 89%~95% highest density intervals (HDIs), $P_{\text{in ROPE}}$, and $P_{\text{above } 0.5}$.
6. **Make decisions with ROPE:**

- If the posterior of $P(i \succ j)$ lies predominantly within $[0.25, 0.75]$ declare i and j practically equivalent (our conservative setting)
- Else if mean $P(i \succ j) > 0.75$ declare i better than j ; if < 0.25 , declare worse.

7. **Aggregate and rank:** Rank models by posterior mean β_i (or by their expected win probability against the field) and report pairwise probabilities alongside the ranking to convey uncertainty.

Additional detailed results

Table 7 shows the complete list of models along with the number of wins or near-wins across the datasets (AUROC < 0.01 from winning score).

Table 6 shows the complete comparison of mean ranks and mean AUROC scores for all tested variants of the models, including all types of classification heads.

In particular, we can see e.g., a clear distinction between MTR and MLM ChemBERTa variants, the former having much better results:

- For the 5M model, the MTR improved the mean rank by 23.5 and the mean AUROC by 7.33%.
- For the 10M model, the MTR improved the mean rank by 16.64 and the mean AUROC by 4.62%.
- For the 77M model, MTR improved the mean rank by 25.14 and the mean AUROC by 9%.

All MTR variants of the ChemBERTa were significantly higher in ranking than any MLM variant.

Pair	Mean	Delta	Above 50%	Within ROPE
CLAMP > ECFP	0.86	0.10	1.00	0.00
Atom Pair > ECFP	0.68	0.17	1.00	0.92
CDDD > ECFP	0.66	0.18	1.00	0.95
ChemBERTa > ECFP	0.60	0.19	0.96	1.00
ECFP > R-MAT	0.72	0.16	1.00	0.74
ECFP > MolBERT	0.79	0.13	1.00	0.19
ECFP > MolFormer	0.80	0.12	1.00	0.11
ECFP > MAT	0.80	0.12	1.00	0.10
ECFP > ChemFM	0.89	0.07	1.00	0.00
ECFP > Mol2Vec	0.94	0.04	1.00	0.00
ECFP > TT	0.94	0.04	1.00	0.00
ECFP > GraphMVP	0.97	0.02	1.00	0.00
ECFP > COATI	0.98	0.01	1.00	0.00
ECFP > Chemformer	0.99	0.01	1.00	0.00
ECFP > MolR	0.99	0.01	1.00	0.00
ECFP > GIN	0.99	0.01	1.00	0.00
ECFP > Uni-Mol2	0.99	0.01	1.00	0.00
ECFP > ChemGPT	1.00	0.00	1.00	0.00
ECFP > GEM	1.00	0.00	1.00	0.00
ECFP > GROVER	1.00	0.00	1.00	0.00
ECFP > Uni-Mol	1.00	0.00	1.00	0.00
ECFP > SimSon	1.00	0.00	1.00	0.00
ECFP > SELFormer	1.00	0.00	1.00	0.00
ECFP > GraphFP	1.00	0.00	1.00	0.00

Table 5: Bayesian Bradley-Terry model statistics for the classification results.

Model Classification head	Mean rank				Mean ROC AUC score			
	best	knn	rf	linear	best	knn	rf	linear
CLAMP	8.84	8.78	9.08	9.58	82.55%	77.77%	81.20%	80.89%
R-MAT [4M]	8.96	9.70	8.78	8.44	80.83%	76.79%	79.96%	79.70%
MolBERT	11.04	10.70	8.94	10.84	80.51%	76.76%	80.19%	78.97%
ChemBERTa [10M][MTR]	11.64	10.17	12.04	14.36	79.99%	76.55%	78.75%	77.91%
ECFP [Count]	11.78	27.04	9.86	17.80	79.89%	71.93%	79.45%	77.05%
CDDD	12.42	11.17	11.16	16.28	80.60%	76.56%	79.77%	77.11%
MAT [2M]	12.70	14.43	13.80	12.62	80.18%	76.25%	79.02%	78.63%
Atom Pair [Count]	13.42	14.04	13.68	18.12	79.48%	75.46%	78.25%	77.20%
ChemBERTa [77M][MTR]	13.86	12.04	13.92	15.28	79.48%	76.13%	78.20%	77.58%
ChemBERTa [5M][MTR]	14.38	10.91	13.88	18.60	79.64%	76.57%	78.46%	77.01%
MAT [20M]	15.00	14.30	16.52	12.44	79.67%	76.06%	78.49%	78.42%
MolFormer	15.42	11.48	15.96	21.28	79.80%	76.09%	78.45%	76.73%
Mol2Vec	16.92	18.22	16.52	17.28	79.55%	74.21%	77.93%	77.83%
ECFP	17.82	25.96	16.00	18.74	78.94%	72.21%	78.39%	76.97%
Atom Pair	18.44	16.65	16.32	18.44	78.60%	74.50%	77.78%	77.11%
MAT [200k]	18.64	23.26	21.26	12.72	79.10%	73.52%	77.62%	78.56%
TT [Count]	20.32	31.78	19.28	25.00	78.08%	70.93%	77.18%	75.43%
TT	21.04	25.48	18.88	22.80	78.12%	72.10%	77.47%	75.90%
ChemFM [3B]	22.48	27.70	33.92	15.36	78.25%	72.73%	74.45%	77.96%
Uni-Mol2	23.76	29.61	27.92	19.40	78.11%	71.61%	75.75%	77.27%
MolR [TAG][1024]	24.20	22.61	23.22	22.04	77.84%	73.83%	76.69%	76.56%
COATI	24.62	23.30	24.00	23.40	78.02%	72.80%	76.95%	76.55%
Chemformer [Mask]	25.68	23.43	26.92	22.28	77.44%	73.26%	75.78%	76.19%
GraphMVP [CP][Max]	26.64	18.35	23.72	35.32	77.18%	74.62%	76.73%	73.05%
GraphMVP [AM][Max]	27.40	28.78	23.20	33.94	77.13%	71.95%	76.89%	73.38%
ChemBERTa [10M][MLM]	28.28	31.61	26.68	29.48	76.46%	71.46%	74.89%	74.24%
Chemformer [Combined]	29.04	28.39	34.40	23.60	76.86%	72.13%	74.05%	76.16%
MolR [GAT][1024]	29.16	29.13	28.38	28.20	76.72%	71.84%	75.83%	75.28%
MolR [SAGE][1024]	29.48	30.91	30.12	27.60	77.04%	71.82%	75.50%	75.45%
MolR [GCN][1024]	30.84	28.39	28.74	28.52	76.59%	72.74%	75.78%	74.94%
ChemFM [1B]	30.96	37.76	39.12	23.64	76.07%	68.95%	72.43%	75.84%
Uni-Mol	31.04	25.65	28.20	26.08	76.85%	72.94%	75.92%	75.98%
GraphMVP [CP][Sum]	32.74	26.78	32.92	33.56	75.58%	72.01%	73.88%	72.61%
GIN [GraphCL][Sum]	33.00	30.83	29.40	35.24	75.14%	70.80%	74.70%	71.64%
GraphMVP [AM][Sum]	33.68	27.28	32.44	35.26	75.29%	71.82%	74.18%	71.83%
GROVER [Large]	34.16	43.30	38.78	30.90	75.68%	66.55%	72.06%	74.97%
Chemformer [Augment]	35.32	40.09	38.68	32.72	75.32%	67.66%	72.87%	74.03%
GROVER [Base]	35.72	41.17	37.32	33.64	75.21%	67.77%	72.55%	73.95%
GraphMVP [CP][Mean]	36.32	31.00	36.48	37.40	74.76%	71.08%	72.87%	71.24%
GraphMVP [AM][Mean]	36.50	30.26	35.48	40.12	74.17%	70.84%	72.96%	69.51%
GIN [Contextual][Sum]	36.60	34.35	34.98	37.56	74.47%	70.11%	73.56%	70.99%
ChemBERTa [5M][MLM]	37.88	37.83	34.66	36.16	74.20%	69.19%	73.64%	72.63%
ChemGPT [19M]	38.38	33.61	37.78	38.36	73.77%	70.84%	72.64%	71.59%
ChemBERTa [77M][MLM]	39.00	40.20	39.14	36.40	72.92%	67.43%	71.28%	71.14%
ChemGPT [4.7M]	39.40	35.13	36.84	40.72	74.01%	70.09%	73.39%	70.99%
SimSon	39.52	33.26	40.16	43.66	73.56%	70.80%	72.15%	69.23%
GEM	39.72	31.57	38.52	39.96	74.03%	71.75%	72.84%	71.42%
GIN [IG][Sum]	41.00	35.02	38.00	43.84	73.08%	69.85%	72.56%	69.34%
SELFormer [Lite]	41.04	38.04	41.92	39.56	73.18%	69.03%	71.57%	70.99%
GIN [Motif][Sum]	41.28	38.70	38.72	43.42	73.21%	68.34%	72.21%	69.21%
GIN [CP][Sum]	44.00	47.17	45.00	40.48	72.08%	65.33%	69.44%	70.54%
SELFormer	44.68	45.13	44.56	41.48	72.14%	66.75%	70.47%	70.74%
GIN [AM][Sum]	45.44	48.65	48.04	40.24	71.31%	64.06%	68.19%	70.09%
GIN [GPT_TNN][Sum]	45.64	45.98	43.44	45.40	71.15%	65.63%	70.04%	66.93%
GIN [EP][Sum]	48.16	46.24	48.48	48.40	64.68%	61.14%	61.16%	61.64%
GraphFP [CP]	53.00	55.13	52.32	53.36	59.67%	50.12%	57.39%	52.67%
GraphFP [C]	54.60	54.52	54.52	55.68	56.11%	49.99%	53.90%	49.70%

Table 6: Full comparison of averaged model performance including all variants and all classification heads.

Model	Number of datasets
CLAMP	14
AtomPair	7
RMAT	6
ECFP	5
ChemBERTa	5
MolBERT	4
CDDD	3
Grover	2
TT	2
Mol2Vec	2
MAT	2
ChemFM	1
MolR	1
GraphMVP	1
MoLFormer	1
SimSon	1
UniMolv1	0
SELFormer	0
COATI	0
ChemFormer	0
GraphFP	0
GIN	0
GEM	0
ChemGPT	0
UniMolv2	0

Table 7: Number of datasets, where a given model won or had a near-win.